BULLETIN OF THE POLISH ACADEMY OF SCIENCES
TECHNICAL SCIENCES, Vol. 69(6), 2021, Article number: e139203
DOI: 10.24425/bpasts.2021.139203

Analysis of the OCHN3MFA steel in terms of cutting forces and cutting material flank wear mechanisms in hard turning processes

Jozef MAJERÍK[2], Igor BARÉNYI[2], Zdenek POKORNÝ[1*], Josef SEDLÁK[3], Vlastimil NEUMANN[4], David DOBROCKÝ[1], Aleš JAROŠ[3], Michal KRBAŤA[2], Jaroslav JAMBOR[2], Roman KUSENDA[2], Miroslav SAGAN[2], and Jiri PROCHÁZKA[1]

[1] Department of Mechanical Engineering, University of Defence in Brno, Brno, Czech Republic
[2] Department of Engineering, Alexander Dubcek University of Trencin, Trencin, Slovak Republic
[3] Department of Manufacturing Technology, Brno University of Technology, Brno, Czech Republic
[4] Department of Combat and Special Vehicles, University of Defence in Brno, Brno, Czech Republic

Abstract. This article deals with the effect of selected machining parameter values in hard turning of tested OCHN3MFA steel in terms of SEM microstructural analysis of workpiece material, cutting forces, long-term tests, and SEM observations of flank wear *VB* and crater wear KT of used changeable coated cemented carbide cutting inserts in the processes of performed experiments. OCHN3MFA steel was selected as an experimental (workpiece) material. The selected experimental steel was analyzed prior to hard turning tests to check the initial microstructure of bulk material and subsurface microstructure after hard turning and chemical composition. Study of workpiece material's microstructure and worn cemented carbide cutting inserts was performed with Tescan Vega TS 5135 scanning electron microscope (SEM) with the X-Ray micro-analyzer Noran Six/300. The chemical composition of workpiece material was analyzed with Tasman Q4 surface analyzer. All hard turning experiments of the used specimens were performed under the selected machining parameters in the SU 50A machine tool with the 8th selected individual geometry of coated cementite carbide cutting inserts clamped in the appropriate DCLNR 2525M12-M type of cutting tool holder. During the hard turning technological process of the individual tested samples made of OCHN3MFA steel, cutting forces were measured with a Kistler 9257B piezoelectric dynamometer, with their subsequent evaluation using Dynoware software. After the long-term testing, other experiments and results were also realized, evaluating the influence of selected machining parameters with different cutting insert geometry on the achieved surface quality.

Key words: mechanical properties; microstructural analysis; cutting forces; flank wear; crater wear.

1. INTRODUCTION

In view of the continuous trend of improving the quality of manufactured parts, it is necessary to ask whether increasing cutting conditions applied to machining affect the properties of the machined surface.

The results of the experiments and the knowledge from the manufacturing practice show us that they certainly do have an effect and a significant one. These changes that occur below the machined surface, caused by deformation and temperature phenomena during the machining process, can have a very negative effect on the functional operation of the components. This demonstrates the need to investigate the state of the subsurface layers and control their properties, especially when components are operating under high stress and require high durability and reliability. The results of scientific publications [1–3] and practical experience show the need to evaluate the condition of the machined surface of these parts as the result of a certain technological process depending on the specific functional conditions of the surface in use. Such a view of the evaluation of the machined surface is nowadays often referred to as surface integrity. Thus, the machining process significantly affects the surface layer of the workpiece and changes its properties. These changes in the surface layer can then be linked to the future functions of the machined surfaces and, thus, used to assess their integrity.

Each finishing technology creates special characteristics on the machined surface and creates a special state thereof. It is the force of the cutting tool that deforms the material leaving in the form of chips and the thin surface layer below the machined surface. The authors [4–6], who were measuring and evaluating individual components of the cutting forces during machining, concluded that with the increase in the hardness of the workpiece when turning high-strength steels, the cutting forces also increase to high values above 50 HRC.

Interaction of the cutting edge with the workpiece during machining results in separating a portion of the material from the workpiece in the form of a chip of different shapes and

*e-mail: zdenek.pokorny@unob.cz

Manuscript submitted 2021-02-22, revised 2021-02-22, initially accepted for publication 2021-08-19, published in December 2021

sizes, including microparticles of the cutting material (from the rake and clearance face of the cutting tool). Of course, this interaction leads to the wear of the tool over time [7, 8]. Wear is the common part of all machine elements that are in contact with each other and their relative movement. The process of tool wear is quite complex, as it depends on many interacting factors (physical and especially mechanical properties of the machined and cutting tool material, type of machining operation, cutting tool geometry, cutting conditions, cutting environment, etc.) and many different physical-chemical activities phenomena (wear mechanism) [9, 10]. Abrasion and adhesion are also often referred to in the technical literature as physical wear mechanisms. Diffusion and oxidation also belong to chemical mechanisms of wear. All these types of wear act smoothly over time so that the time of onset of their action may not always be the same. Plastic deformation and brittle fracture, on the other hand, are mechanisms that act suddenly at some point and usually cause immediate termination of the tool's functionality (sudden change in the tool's cutting-edge shape, avalanche wear, or tip peeling) [11, 12].

The clearance face of the cutting tool wears mainly due to abrasion and oxidation, while the rake face wears due to adhesion, diffusion, abrasion, and oxidation. Various performed experiments of the collective of authors show [13, 14] that the cutting-edge wears mainly on the clearance and rake face of the cutting tool or the tip itself. The size of the individual wear is thus dependent on the contribution of certain co-operating factors of the cutting process, such as cutting tool geometry, type of machining operation (roughing, finishing) and, last but not least, also cutting conditions such as cutting speed v_c $\left(\text{m.min}^{-1}\right)$, feed rate f $\left(\text{mm.rev}^{-1}\right)$, depth of cut a_p (mm).

Various authors investigated the effect of various machining parameters on cutting tool wear in the machining process of metallic materials with defined geometry of cutting tool was investigated by various authors, and their investigations were published in papers [15–17].

The most used criterion for determining the guaranteed tool wear of the changeable cutting insert is the wear of the cutting edge shown on its n clearance face, indicated by the letters *VB*. It is a length parameter (perpendicular to the plane of the face) of the newly formed surface due to the removal of the cutting material from the clearance face of the cutting edge. This wear greatly affects heat generation during the cutting process and the final roughness of the resulting surface after the machining process. This tool surface is in contact with the machined surface all the time. Therefore, diffusion processes can occur on the surfaces of both materials. Subsequently, the composition of the surface layers of the cutting and the machined material affects the interaction.

The main aim of the authors' research was to determine the impact of force load on the cutting tool while implementing the so-called short-term machining tests using the piezoelectric dynamometer Kistler. Subsequently, the size and method of wear on the *VB* on the cutting tools' clearance face were analyzed by carrying out the so-called long-term machining tests. The resulting wear of *VB*, its shape and size were examined by SEM microscopy.

2. EXPERIMENTAL WORK

2.1. Workpiece material characterization

The experimental material that was the basis of the research carried out by the authors' team is also referred to as OCHN3MFA steel. In practice, it is a type of medium-alloy steel, and its use is mainly in the special engineering industry. The steel is supplied in a rod form, first cast and then further technologically processed by forging. From the point of view of heat treatment, it is remelted in a vacuum. In the process of their experiments, the authors used a CCD-based Q4 TASMAN emission spectrometer in order to determine the chemical composition of the experimental material. The measured values of the chemical composition can be seen in Table 1. In terms of chemical affinity and the equivalents of this steel used, for example, 35NiCrMoV12-5 steel or AISI 4340 steel according to the American standard is used.

Table 1
Chemical composition of OCHN3MFA examined steel

	C	Mn	Si	Cr	Ni	Mo	V
Min	0.33	0.25	0.17	1.20	3.00	0.35	0.10
Max	0.40	0.50	0.37	1.50	3.50	0.45	0.80
Spectral analysis	0.41	0.55	0.38	0.92	2.85	0.22	0.13

In addition to the chemical composition, the authors measured the mechanical properties of the tested steel. The Instron Wolpert HV5 experimental device with a load of $F = 49.03$ N and a holding time $t = 10$ seconds was used for this purpose. According to the EN ISO 6892-1 standard, the authors performed a tensile test, and according to the EN ISO 179-1 standard, an impact test was performed on a Charpy hammer. The measured values from the above tests can be seen in Table 2.

Table 2
Mechanical properties of OCHN3MFA examined steel

Mechanical properties	Tensile strength R_m (MPa)	Limit of proportionality R_E (MPa)	Toughness KCU (J) at 20°C	Hardness (HV)	Elongation A_5 (%)
	1500	1079	23	500	20

Microstructural analysis of the base material of the investigated steel was performed using a SEM Tescan Vega TS 5135 with a Noran Six/300 X-ray microanalyzer and an Oxford Instruments MFP-3D Infinity AFM microscope, but AFM only in the previous part of the authors' investigation. The SEM method was used based on the electron properties of waves and is analogous to conventional light microscopy. Authors have already published the results obtained for AFM analysis of the investigated steel. Barényi *et al*. [18].

2.2. Turning process and machining parameters

In the planned process of experiments, it was necessary to carry out the so-called short and long-term cutting tests for OCHN3MFA barrel steel. The workpiece material was in bar form with dimensions of Ø60 mm and length $l = 900$ mm. Subsequently, in the processes of performed experiments, the workpiece was longitudinally turned under specified cutting conditions to monitor both the force load and the tool wear of the cutting edges on selected changeable carbide cutting inserts. All selected inserts with letters from A (designated as CNMG120408-M5 according to ISO standard), B (CNMG120412-M5), C (CNMG120408-M5), D (CNMG 120408-M6), E (WNMG080408-M5), F (WNMG080408-M3), G (WNMG080412-M3) up to H (WNMG080408-M5) were sequentially tested under the same cutting conditions for each insert. For each tested insert, a total of 12 individual passes of 180 mm in length were performed on the prepared workpiece test material.

Cutting tests were carried out on a universal SU 50 A/1500 lathe machine with an additional speed sensor to turn medium-sized workpieces precisely. It enables the use of carbide cutting tools and thread cutting over a wide pitch range. Two electric motors drive the working spindle via a transmission clutch.

The same eight types of changeable cutting inserts with different geometries were also used for external longitudinal turning of OCHN3MFA barrel steel or so-called short-term tests. The set cutting conditions for both tests (see Table 3) were the same for all tested inserts.

Table 3
Set values of cutting conditions in experimental processes

Workpiece diameter D (mm)	Depth of cut a_p (mm)	Number of cut 1 to 12 (–)	Feed rate f (mm)		Spindle speed n (min^{-1})	Cutting speed v_c (m.min^{-1})
60	1	1	$f1$	0.22	950	180
58		2			990	
56		3			1020	
54		4	$f2$	0.25	1060	
52		5			1100	
50		6			1140	
48		7	$f3$	0.34	1190	
46		8			1240	
44		9			1300	
42		10	$f4$	0.41	1360	
40		11			1430	
38		12			1500	

The priority of the performed tests was to machine at a constant cutting speed; hence, with the decreasing diameter of the test rod (workpiece) the spindle speed increased as well. The depth of cut a_p (mm) was chosen to be 1 mm. The cutting speed v_c (m.min^{-1}) was set to 180 m.min^{-1}; thus, the highest possible cutting speed was selected with respect to the type of machine tool used.

Therefore, the same cutting tools from the Seco Tools CZ Company were chosen for long-term cutting tests, namely two cutting insert geometries in several designs. A total of 8 types of cutting inserts were also subjected to cutting tests, while the cutting tool material was also used along with TP0501 sintered carbide, as in the short-term tests.

2.3. Measurement of cutting forces

The main monitored parameter at testing all types of cutting inserts was the force load during longitudinal turning. The force load was measured for each pass at each insert. For this purpose, a piezoelectric dynamometer KISTLER type 9257B was used instead of standard knife support. The signal from the dynamometer is transmitted by means of a connecting cable to the distribution box, from which it goes further to the KISTLER 5070A charge amplifier. The amplifier is connected to a notebook that displays the resulting loads using Dynoware software. The sample rate was set to 3000 Hz, up to two times the machine's maximum spindle speed. Using the Dynoware evaluation software, graphs of the Fi force components as a time t (min) function were then created.

The first cut of the tool always began at the initial bar diameter of Ø60 mm, while the last passage was at the diameter of Ø38 mm. To maintain a constant surface cutting speed, the spindle speed had to be constantly increased due to the decreasing cutting diameter. This was also reflected in the times of individual cuts, with the first cut lasting the longest time and the last cut being considerably shorter (due to increasing revolutions). As a result, graphs of force load versus time with a different timeline on the x-axis for individual cuts have been generated.

All three components of the force load (cutting forces Fc, passive forces Fp and feed forces Ff) were also measured and exported to an Excel editor. By using all these components, the total cutting force F was then calculated. The x-axis represents the value of the individual acting force components, from which the resulting force was calculated as the total acting force F. Therefore, the x-axis, which represents time, is set as a constant axis for better clarity. Due to the fact that machining was performed at a constant surface cutting speed, the spindle speed increased with decreasing workpiece diameter. Thus, the machine time was reduced with increasing spindle speed and feed rate. The measured data were filtered in Matlab and then transferred to the Excel editor. The obtained force components, including the total cutting force, were then plotted into force graphs over time.

2.4. Measurement of flank wear

The performed experiments of the author were also determined as the characteristics of the material tested and the material of selected cutting tools, especially the flank wear VB in all tested types of cutting inserts. After every second tool cut, the flank wear criterion VB was measured using a workshop microscope. Graphical dependence of flank wear criterion VB

on turning time t (min) was then expressed from the obtained data. Conclusions were drawn directly from the measured data, and subsequently, the most suitable types of cutting inserts for machining the tested barrel steel were determined. The cutting insert marked with the letter A was tested first. 12 passes of 100 mm length were always performed (3 passes for each of the four-set feed rate values). The monitored parameter included mainly the force load during the longitudinal turning of the tested barrel steel. All cutting tools were tested in the same way (cutting insert marked A up to the cutting insert marked H).

The standard procedure involves determining the value of the flank wear criterion *VB* and consequently reaching it. The cutting tool is evaluated as worn. Hence, the tool life means the time when a predetermined value of flank wear *VB* has been reached. After all the passes have been performed for each tested cutting insert, the total amount of flank wear *VB* achieved at the end of testing is then determined. Thus, the machining time is the same for all tested cutting inserts, and the difference is only in the amount of flank wear *VB* at the end of the long cutting tests.

3. RESULTS AND DISCUSSION

The following results were obtained based on their microstructural analysis of the workpiece material, which the authors have already published in their article [18]. The authors of the article evaluated the microstructure of the basic material of the investigated steel and used SEM microscopy in this article and AFM microscopy in the first phase of their research. Microscopic analysis shows that the microstructure of the investigated steel is relatively coarse-grained and consists of highly tempered martensite and bainite with fine globular carbides. The original austenitic grain had a mean size of about 50 micrometers.

The average size of the original austenitic grain (grains after the last austenitizing) was about 50 μm, as seen in Fig. 1.

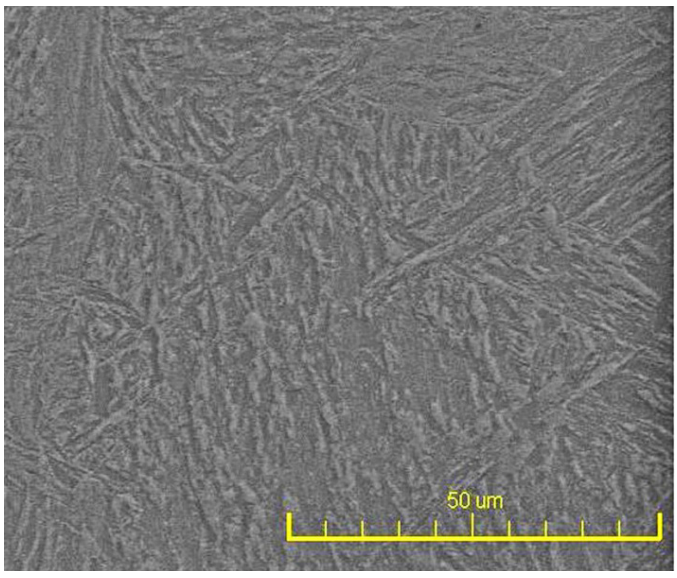

Fig. 1. Microstructure of the examined OCHN3MFA steel, bulk material, etch Nital

In the process of experiments, the authors found that the microstructure of the basic material corresponds to the state after hardening and high-temperature tempering of coarse-grained Cr-Ni-Mo-V steels. From the point of view of examining the machined surface, the layer affected by the technological process visible on the SEM image was visible, as can be seen from the SEM image in Fig. 2.

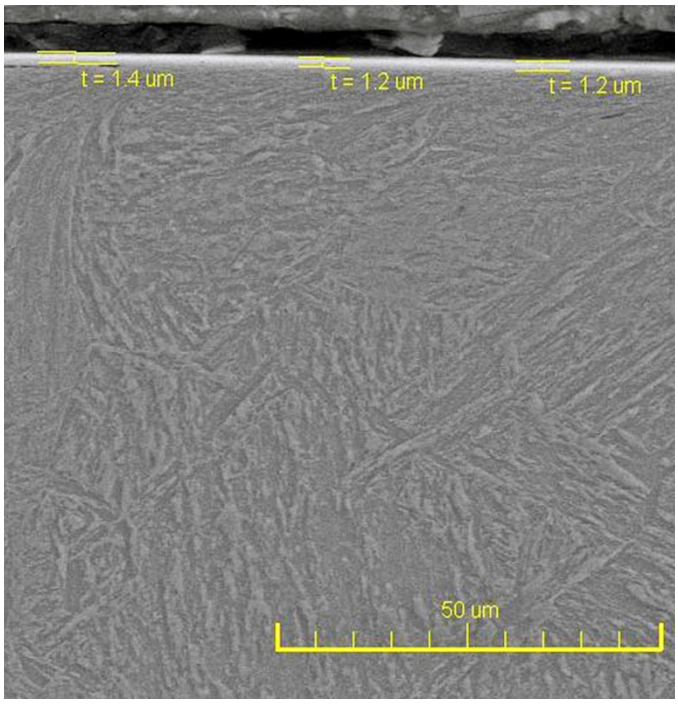

Fig. 2. Surface microstructure of the examined OCHN3MFA steel after hard turning, also known as Bielby, etch Nital

In the first phase of the experiments performed by the authors of the article, analysis of the force load at external longitudinal turning was carried out. Graphical dependencies were created from the data obtained during the longitudinal turning of the tested steel for all tested tools. It is apparent from the measured data that the machine time has been reduced with increasing feed rate and spindle speed. It is also evident from the graphical dependencies that all the acting force components increased with a higher feed rate per revolution. It can be said that the increase in total applied force F was about 1.5 times greater when compared between the feed rates f_1 and f_4, as can also be seen from Fig. 3.

It can be seen from the total measured load values (Fig. 3) that there was no significant increase in force values. Visible increases can only be observed with inserts marked E and F, showing a slight increase in the total cutting force F between the first and last pass. As for the other types of cutting inserts, there was no increase between the first and the twelfth cut, but the initial load values were reduced and stabilized. To provide a better overview, Fig. 3 shows an overall comparison of the mean values of the cutting force Fc component for all tested types of cutting inserts for the first and the last cut. For this

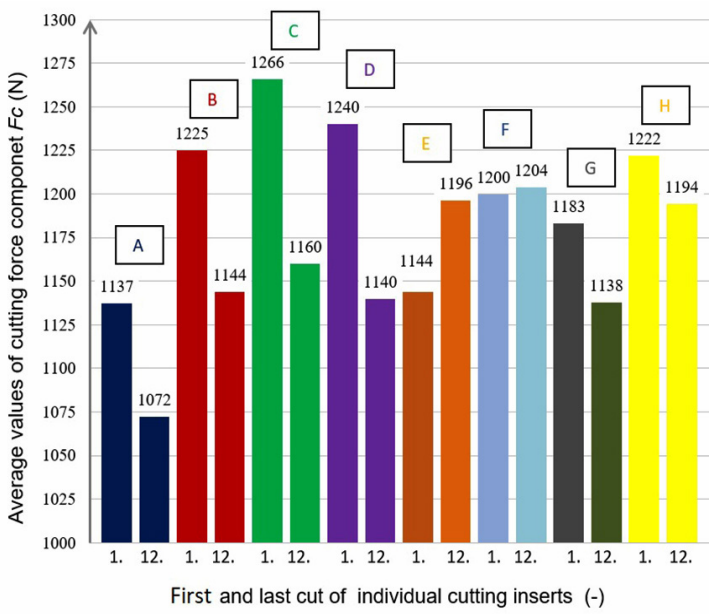

Fig. 3. Comparison of *Fc* cutting forces mean values

reason, Figs. 4 to 7 also show the highest average values of the total cutting force at the first and the last cuts for the cutting insert G, as well as the smallest values recorded for the cutting insert, marked F. In some cases, with several cutting tools tested, there has been a gradual decrease in total force *F*, which is due to the fact that some cutting tools (with different geometries) need to be run first, which means that this is a run-in wear. As for the next phase of testing, when all inserts have been cut for an extended period of time, all of the acting force components will gradually increase during the testing process.

Data obtained from all the performed short-term tests thus suggest choosing the value of feed rate per revolution at $f = 0.34$ mm as most appropriate because of the most stable cutting forces components in most tested cutting tools.

Short-term test data obtained from the longitudinal turning of the tested OCHN3MFA steel were also used to construct the so-called box plots for the cutting value *Fc* for all tested inserts at all four set feed rates. In order to compile the following graphs, the entry and exit of the cutting tool from / to the workpiece have not been taken into account to make the statistics more meaningful. An example is a statistical representation of

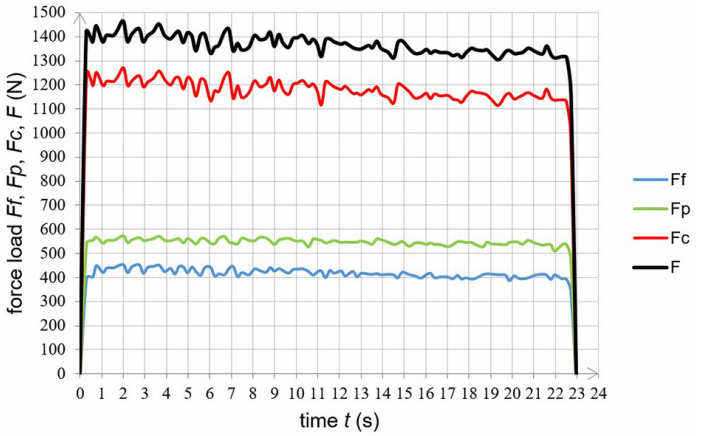

Fig. 4. Graphical dependence of the force load of the first pass of the insert marked with the letter G, dependent on the machining time

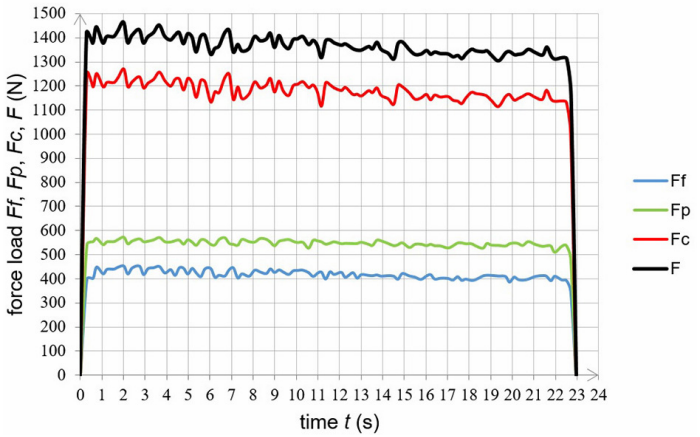

Fig. 5. Graphical dependence of the force load of the last pass of the insert marked with the letter G on the machining time

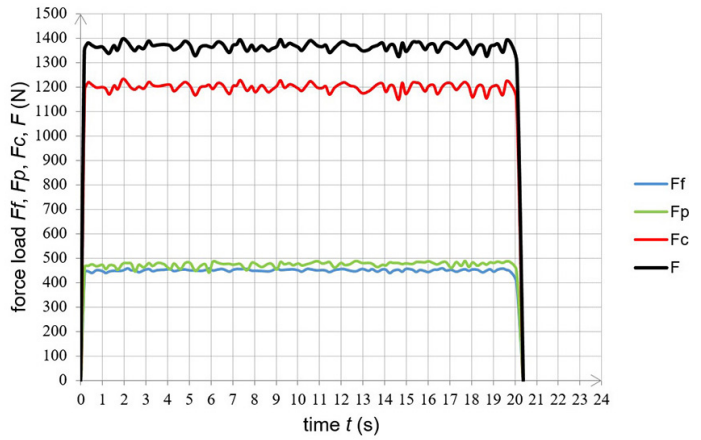

Fig. 6. Graphical dependence of the force load of the first pass of the insert marked with the letter F on the machining time

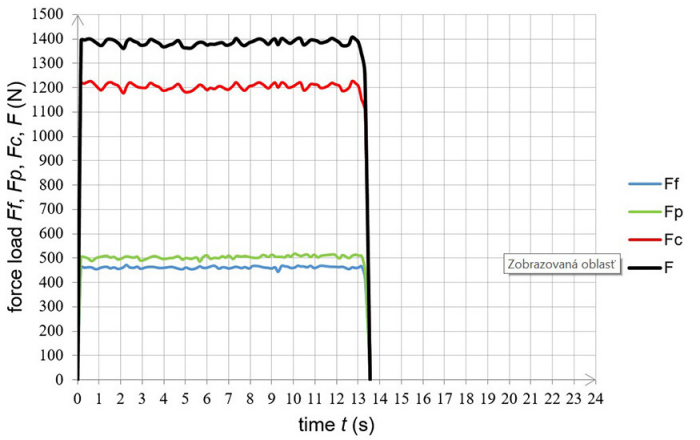

Fig. 7. Graphical dependence of the force load of the last pass of the insert marked with the letter F on the machining time

the data obtained with changeable cutting inserts marked with the letter G, recording the highest average values of the total cutting force measured at the last cut, compared with cutting inserts of the lowest force load values recorded with F inserts. Statistical evaluation of Figs. 8 and 9 suggests that most of the measured values during machining fall within a closed area, with only a few outliers and extremes. The graphs also show the evolution trend, so that with increasing set feed rate per revolution, there was a gradual increase in cutting force *Fc* for all tested cutting inserts.

For the best and worst tested carbide cutting insert, graphical dependencies of the first and the last twelfth cut are also shown to illustrate how the force load changes with increasing flank wear on the cutting insert. It is not necessary to graphically compare all the measured dependencies of each cut for all types of tested cutting inserts since the differences between the individual force loads are practically very small due to the small difference in flank wear between them.

The measured curves of flank wear according to *VB* criterion as a function of the cut number for all the tested cemented carbide cutting inserts marked from A to H are shown in Fig. 10.

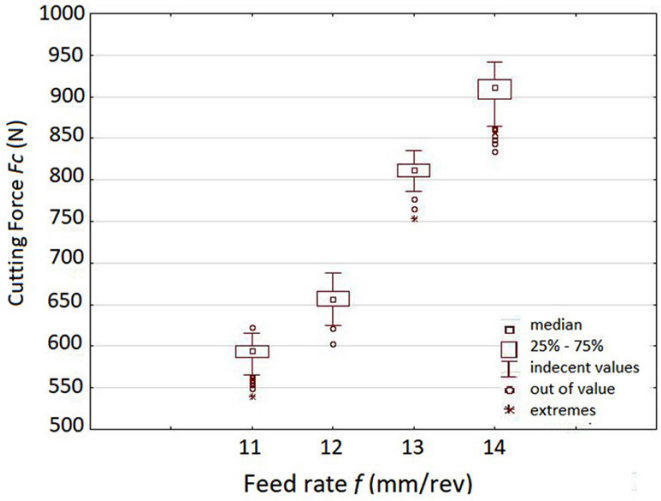

Fig. 8. Statistical comparison of the measured cutting force values *Fc* as a function of the feed rate *f* for the tested cutting insert marked G with the highest measured average values of the total cutting force at the last cut

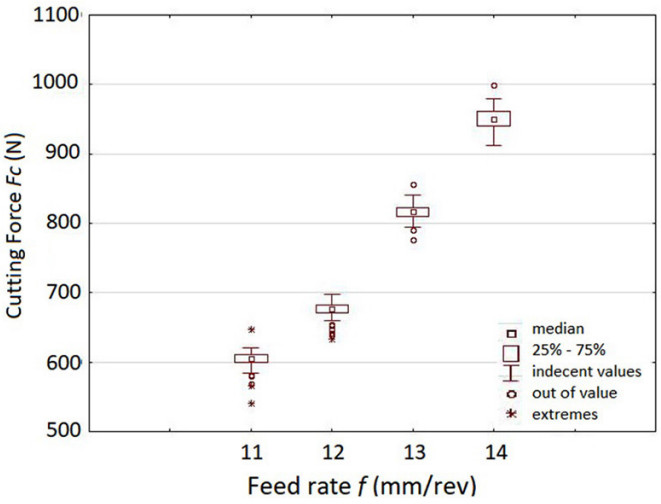

Fig. 9. Statistical comparison of measured values of cutting force Fc as a function of feed rate *f* for the tested cutting insert marked F with the lowest measured average values of total cutting force at the last cut

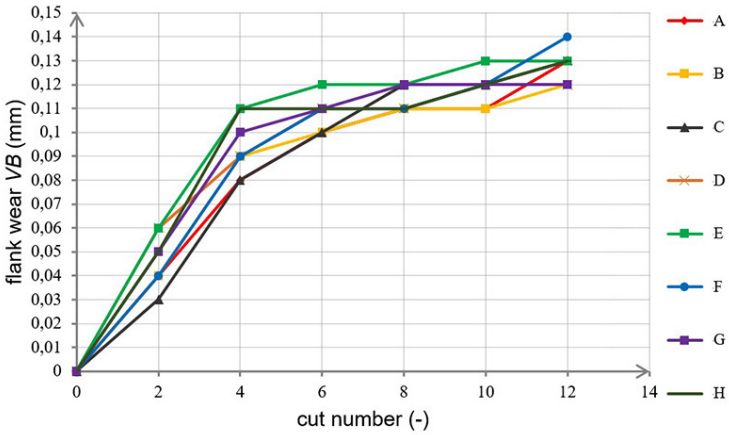

Fig. 10. Graphical dependence of mutual comparison of individual flank wear *VB* for all types of tested cutting inserts marked from A to H on the cut number

All achieved wear figures of the tested cutting inserts from the graph dependencies in Fig. 10 are very similar. As shown in the short-term tests, the greatest wear can be observed in the cutting insert marked with the capital letter F. On the contrary, the most favourable course of flank wear can be observed for the cutting insert marked with the letter G. For this reason, Fig. 11 to 13 show SEM electron microscope images of flank wear *VB* and, particularly, a crater wear *KT* of the best G-marked cutting insert after long-term cutting tests.

After the finished cutting tests, all the tested cutting inserts were analyzed by SEM electron microscopy. However, although the results are very similar, here we only present the figures for the cutting insert that achieved the best results. From the photographs, the main mechanisms of wear included abrasion

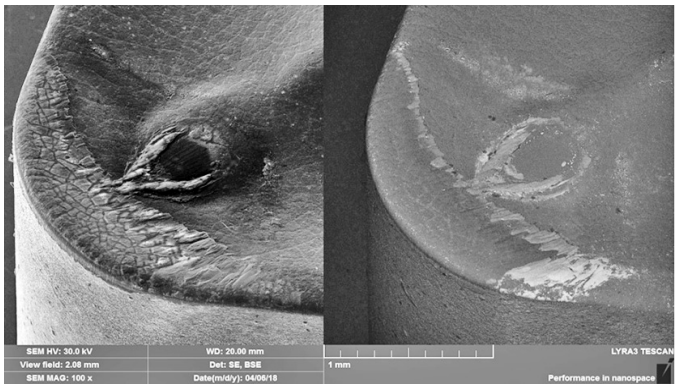

Fig. 11. SEM image of the flank and rake surfaces of G-marked carbide cutting insert observed through a Tescan Lyra electron microscope

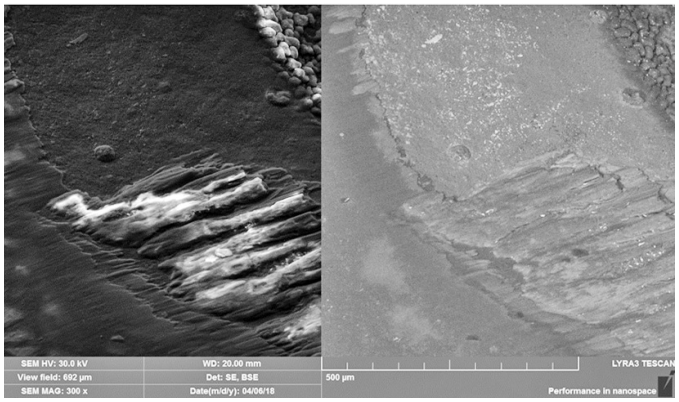

Fig. 12. SEM image of the G-marked carbide cutting insert with visible area of crater wear *KT* on rake face observed through a Tescan Lyra electron microscope

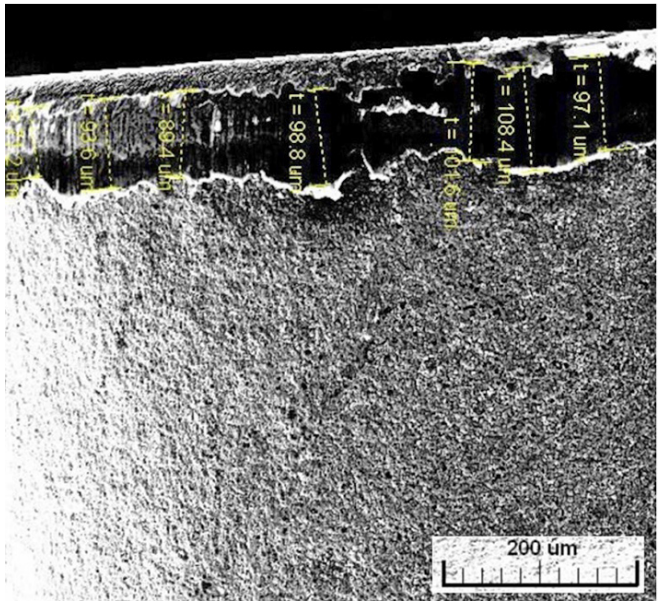

Fig. 13. SEM image of flank area appearance with marked numerical values of *VB* wear size (cutting insert marked as G, with geometry WNMG080412) observed through a Tescan Vega electron microscope

and adhesion. Also, the main observed effect was the amount of flank wear *VB* (Fig. 13). Also, yet to a lesser extent, crater wear *KT* was observed (Fig. 12). The image is formed by detecting secondary and backscattered electrons emitted from the particle beam impact site. Furthermore, it can be observed that the coating has not been removed, possibly due to the shorter machining time.

4. CONCLUSION

The first phase of the experimental part, in addition to the study of microstructure and basic mechanical properties of the tested steel, involved measuring the force load of all tested types of cutting tools during turning. Subsequently, in the second phase of the experiment, the wear of the cutting tools, so-called long-term testing, was also monitored. At the end of the long-term cutting tests, we evaluated and processed all measured data from the obtained force load curves and flank wear analysis of the tested cutting inserts. The experiments were completed by making an overall evaluation of the achieved results, followed by the final choice and the recommendation as to the most suitable insert for turning the tested steel. Thus, all the performed experiments aimed to select the most suitable type or types from the total set of tested cutting inserts, depending on the wear and force load during machining of the tested OCHN3MFA steel.

Consequently, the subsequent results of performed experiments show:

- machine time for all tested cemented carbide inserts was $t_s = 5{,}45$ min,
- as the diameter of the machined workpiece decreases, the value of the cutting speed is subsequently reduced, and to maintain a constant surface cutting speed at a reduced diameter of the material to be machined, the cutting speed must then be increased,
- from the data obtained from short-term cutting tests, it seems that the feed per revolution of $f = 0.34$ mm is most suitable, precisely due to the most stable course of force components in most of the tested carbide cutting inserts,
- the smallest average cutting force values at the last cut were recorded for the cutting inserts marked as B, D and G,
- the highest average cutting force values at the last cut were recorded for the cutting insert marked F,
- the smallest average value of cutting force *Fc* was reached with the cutting insert marked A,
- the highest average values of cutting force *Fc* in the last cut were reached by the cutting insert marked F,
- the lowest flank wear according to the predetermined wear criterion *VB* was achieved by the cutting insert marked B, D and with G ($VB = 0.12$ mm),
- the highest flank wear according to the wear criterion *VB* was achieved with the cutting insert marked F ($VB = 0.14$ mm),
- based on all the performed experiments, the G insert (geometry WNMG080412) appears to be the most suitable cutting insert for turning of the tested steel,
- the least suitable of all submitted carbide cutting inserts in terms of the results of all tests performed is the cutting insert marked F (geometry WNMG080408-M3).

Examining the wear of cutting materials in the form of various studies and selected types of individual experiments at varying cutting parameters helps us better understand the processes occurring in the interaction of the cutting material with the tested steel as a workpiece. This knowledge leads us to determine certain new hypotheses and conclusions. These phenomena then allow us to analyze, solve and define the following actions leading to the reduction of negative impacts on the structure of either the cutting material or the machining process itself. This also ultimately leads to an increase in either the cutting performance or the tool life. However, developing new types of wear-resistant cutting materials with high cutting parameters is a very complex, costly, and time-consuming process. At present, it is unlikely that new cutting materials will be developed in the near future, with properties such as tool life of

cutting edge or range of applications that will be significantly higher than the properties of cutting materials used today. However, with intensive and sustained research and the subsequent refinement of existing cutting materials, we can improve their overall properties in terms of their increased performance or tool life. Another trend to improve the properties of current cutting materials is the development of multilayer surface coatings for cutting tools and changeable cutting inserts, with continuing innovations of new types of coatings that effectively increase the cutting edge's tool life.

ACKNOWLEDGEMENTS

This work was supported by the Slovak Research and Development Agency under contract No. APVV-15–0710 and by the Brno University of Technology, Faculty of Mechanical Engineering, Specific research 2019, with the grant "Research of perspective production technologies", FSI-S-19–6014, as well as by University of Defence in Brno by the Research Project for the Development of the Organization "DZRO Military autonomous and robotic systems".

REFERENCES

[1] G. Sun, R. Zhou, J. Lu, and J. Mazumder, "Evaluation of defect density, microstructure, residual stress, elastic modulus, hardness and strength of laser-deposited AISI 4340 steel," *Acta Mater.*, vol. 84, pp. 172–189, 2015, doi: 10.1016/j.actamat.2014.09.028.

[2] A.K. Sahoo and B. Sahoo, "Experimental investigations on machinability aspects in finish hard turning of AISI 4340 steel using uncoated and multilayer coated carbide inserts," *Measurement*, vol. 45, no. 8, pp. 2153–2165, 2012, doi: 10.1016/j.measurement.2012.05.015.

[3] R. Lalbondre, P. Krishna, and G.C. Mohankumar, "Machinability Studies of Low Alloy Steels by Face Turning Method: An Experimental Investigation," *Procedia Eng.*, vol. 64, pp. 632–641, 2013, doi: 10.1016/j.proeng.2013.09.138.

[4] Ş. Baday, H. Başak, and A. Güral, "Analysis of spheroidized AISI 1050 steel in terms of cutting forces and surface quality," *Met. Mater.*, vol. 54, no. 05, pp. 315–320, 2016, doi: 10.4149/km_2016_5_315.

[5] R. Meyer, J. Köhler, and B. Denkena, "Influence of the tool corner radius on the tool wear and process forces during hard turning," *Int. J. Adv. Manuf. Technol.*, vol. 58, no. 9–12, pp. 933–940, 2011, doi: 10.1007/s00170-011-3451-y.

[6] M.S.H. Bhuiyan, I.A. Choudhury, and M. Dahari, "Monitoring the tool wear, surface roughness and chip formation occurrences using multiple sensors in turning," *J. Manuf. Syst.*, vol. 33, no. 4, pp. 476–487, 2014, doi: 10.1016/j.jmsy.2014.04.005.

[7] L.H. Maia, A.M. Abrao, W.L. Vasconcelos, W.F. Sales, and A.R. Machado, "A new approach for detection of wear mechanisms and determination of tool life in turning using acoustic emission," *Tribol. Int.*, vol. 92, pp. 519–532, 2015, doi: 10.1016/j.triboint.2015.07.024.

[8] A. Cakan, F. Evrendilek, and V. Ozkaner, "Data-driven simulations of flank wear of coated cutting tools in hard turning," *Mechanics*, vol. 21, no. 6, 2016, doi: 10.5755/j01.mech.21.6.12199.

[9] W.B. Rashid, S. Goel, J.P. Davim, and S.N. Joshi, "Parametric design optimization of hard turning of AISI 4340 steel (69 HRC)," *Int. J. Adv. Manuf. Technol.*, vol. 82, no. 1–4, pp. 451–462, 2015, doi: 10.1007/s00170-015-7337-2.

[10] G. Bartarya and S.K. Choudhury, "State of the art in hard turning," *Int. J. Mach. Tools Manuf.*, vol. 53, no. 1, pp. 1–14, 2012, doi: 10.1016/j.ijmachtools.2011.08.019.

[11] W. Jiang and A.P. Malshe, "A novel cBN composite coating design and machine testing: A case study in turning," *Surf. Coat. Technol.*, vol. 206, no. 2–3, pp. 273–279, 2011, doi: 10.1016/j.surfcoat.2011.07.008.

[12] B.D. Beake, J.F. Smith, A. Gray, G.S. Fox-Rabinovich, S.C. Veldhuis, and J.L. Endrino, "Investigating the correlation between nano-impact fracture resistance and hardness/modulus ratio from nanoindentation at 25–500°C and the fracture resistance and lifetime of cutting tools with $Ti_{1-x}Al_xN$ ($x = 0.5$ and 0.67) PVD coatings in milling operations," *Surf. Coat. Technol.*, vol. 201, no. 8, pp. 4585–4593, 2007, doi: 10.1016/j.surfcoat.2006.09.118.

[13] A. Cakan, "Real-time monitoring of flank wear behavior of ceramic cutting tool in turning hardened steels," *Int. J. Adv. Manuf. Technol.*, vol. 52, no. 9–12, pp. 897–903, 2010, doi: 10.1007/s00170-010-2793-1.

[14] J. Jaworski and T. Trzepieciński, "Research on durability of turning tools made of low-alloy high-speed steels," *Met. Mater.*, vol. 54, no. 1, pp. 17–25, 2016, doi: 10.4149/km_2016_1_17.

[15] W. Zebala, "Tool stiffness influence on the hosen physical parameters on the milling process," *Bull. Pol. Acad. Sci. Tech. Sci.*, vol. 60, no. 3, pp. 597–604, 2012, doi: 10.2478/v10175-012-0071-0.

[16] P. Raja, R. Malajamuthi, and M. Sakthivel "Experimental investigation of cryogenically treated HSS tool in turning AISI1045 using fuzzy logic Taguchi approach," *Bull. Pol. Acad. Sci. Tech. Sci.*, vol. 67, no. 4, pp. 687–696, 2019, doi: 10.24425/bpasts.2019.130178.

[17] J. Waszko, "Laser surface remelting of powder metallurgy high speed steel," *Bull. Pol. Acad. Sci. Tech. Sci.*, vol. 68, no. 6, pp. 1425–1432, 2021, doi: 10.24425/bpasts.2020.135385.

[18] I. Barényi *et al.*, "Material and technological investigation of machined surfaces of the OCHN3MFA steel," *Met. Mater.*, vol. 57, no. 02, pp. 131–142, 2020, doi: 10.4149/km_2019_1_131.